

# Thermal Stability Studies of Transparent Conducting Polyaniline Composite Films on Their Conductivity and Optical Spectra

SUNG WEON BYUN and SUNG SOON IM\*

Department of Textile Engineering, College of Engineering, Hanyang University, Seoul 133-791, South Korea

## SYNOPSIS

The thermal stability of highly transparent and conducting polyaniline–Nylon 6 (PAN-N) composite films doped with various protonic acids such as hydrochloric acid (HCl), benzenesulfonic acid (BSA), sulfosalicylic acid (SSA), and *p*-toluenesulfonic acid (TSA) was investigated at different elevated temperatures under air atmosphere. Two different degradation kinetic processes of electrical conductivity were found depending on the species of protonic acids. The conductivity degradation of PAN-N composite films doped with SSA and TSA were found to obey first-order reaction kinetics, while that of the other dopants was found to follow multiorder kinetics. Spectroscopic studies revealed that the thermal de-doping process of doped composite films, which reversed the doping process, took place without major structural modifications of the polyaniline in the composite system but was not completely reversible. From the differential scanning calorimetry (DSC) study, the crystal structure of the composite films was found to be affected by the formation of polyaniline in matrix polymer and depended on the types of dopant species. © 1995 John Wiley & Sons, Inc.

## INTRODUCTION

Polyaniline has been extensively studied because it exhibits good environmental stability and its electrical properties can be modified by both the oxidation state of the main chain and protonation.<sup>1–6</sup> The wide range of associated electrical and optical properties, coupled with good stability, make polyaniline attractive as an electronic material for potential use in a variety of applications.<sup>7–10</sup> However, the issue of stability still remains as one of the major drawbacks to the development of conducting polyaniline. The thermal stability of conducting polyaniline will clearly play a key role in determining the types of applications appropriate for this material. Recently, many researchers have investigated the dopant dependence on the thermal stability of polyaniline.<sup>11–13</sup> However, until now, only a few stability-related studies on its composite forms have been reported.

From our previous work,<sup>14,15</sup> it was found that highly transparent and conducting Nylon-6-based composite films could be easily obtained from polyaniline using a diffusion–oxidation process. The diffusion behavior of monomers in the polymer matrix and the optimum reaction conditions of these composite films was investigated, and the effects of the preparative conditions on the conductivity, transmittance, and mechanical properties of these composite films were studied.

The objectives of this study are to report on the investigation of the thermal stability of transparent, conducting polyaniline composites and the role of the dopant in degradation and to study the kinetics of degradation of conductivity in these composite systems. In order to gain an understanding of the conductivity degradation kinetics of doped composite films, the conductivity stability of a series of composite films with different dopants (including both inorganic and organic acids) were investigated. The conductivity of the as-prepared doped composite films was continuously monitored at different elevated temperatures in air. The composite films

\* To whom correspondence should be addressed.

were also examined by ultraviolet–visible spectroscopy in order to probe the nature of the changes occurring during thermal treatment.

## EXPERIMENTAL

### Preparation of Transparent and Conducting PAN-N Composite Films

Highly transparent and conducting polyaniline–Nylon 6 (PAN-N) composite films were prepared by immersing Nylon 6 films containing aniline monomer into the oxidant solution (aqueous ammonium peroxydisulfate solution) containing various protonic acids such as hydrochloric acid, benzenesulfonic acid, sulfosalicylic acid, and *p*-toluenesulfonic acid. Details of these preparation procedures can be found in the previous papers.<sup>14,15</sup> The concentrations of the oxidant and protonic acid solution were 0.025 and 1 mol %, respectively. The polymerization temperature and time were 4°C and 2 h, respectively. Shiny, pale green-colored films were obtained with a thickness of 20  $\mu\text{m}$  and conductivities and transmittances were about  $10^{-1}$  order (S/cm) and 75% (at 500 nm), respectively. The as-prepared doped composite films were converted to the de-doped forms (emeraldine base form of polyaniline) by treatment with 0.5 mol % aqueous KOH solution for 2 h. The re-doping experiment, after thermal treatment, was performed in each aqueous protonic acid solutions (1 mol %) for 24 h at room temperature.

### Measurements

The conductivity of the composite films was measured using the standard four-probe method, and the ultraviolet–visible absorption spectra of composite films were recorded with UNICAM 8700 series UV/VIS spectrophotometer. Differential scanning calorimetry (DSC) studies were performed on a DuPont 2100 V 4.1 C system under nitrogen atmosphere, programmed heating rate being 10°C/min.

## RESULTS AND DISCUSSION

### Thermal Stability of the Electrical Conductivity

Many investigators have observed the effect of dopant on the physical properties of conducting polymers, and it has been reported that the thermal

stability and mechanical properties of the conducting polymer may be influenced by the choice of anion.<sup>16–18</sup> Previous studies suggested that chemical differences between the anions could be responsible for the anion-dependent properties. We have examined the kinetics of the degradation process of a polyaniline composite system doped with a variety of anions in order to identify different degradation pathways for the degradation of electrical conductivity in a polyaniline composite system as a function of anion in air.

Figures 1–4 show the conductivity stability of various doped PAN-N composite films at different elevated temperatures in air. The data are plotted as a function of  $\log[\sigma_t/(\sigma_0 - \sigma_t)]$  vs. time (min).  $\sigma_t$  and  $\sigma_0$  represent the conductivities of the composite films at the temperature of the experiment at a given time and at time zero, respectively. Generally, the conductivities of all doped PAN-N composite films decay at elevated temperature in air, with the loss in conductivity being most pronounced at 150°C or higher, which is above both the glass transition temperature of the matrix polymer and the dissociation temperature of the dopants.<sup>13,19</sup> It seems that the conductivity decrement of the composite films is due to both the dissociation of dopants and the destruction of the conduction network by the difference of degree of thermal expansion between polymer matrix and polyaniline. The conductivity degradation rate constants, as well as the apparent activation energies, were calculated from the curve slopes using the data collected after 100 or 60 min and an Arrhenius analysis.<sup>18</sup> The results of this kinetics analysis using the following equations are tabulated in Table I:

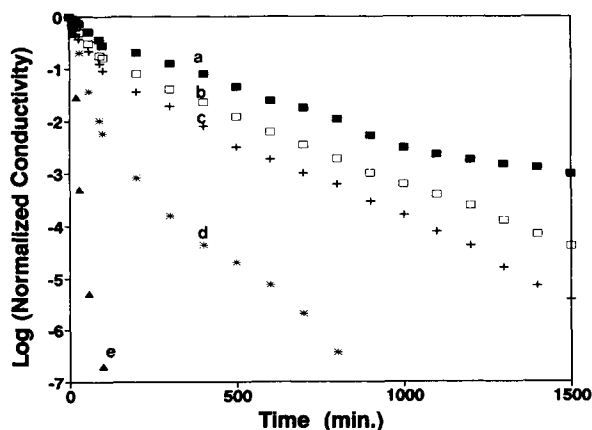


**Figure 1** Conductivity stability of HCl-doped PAN-N composite films at elevated temperatures: (a) 80°C, (b) 95°C, (c) 110°C, (d) 125°C, and (e) 150°C.

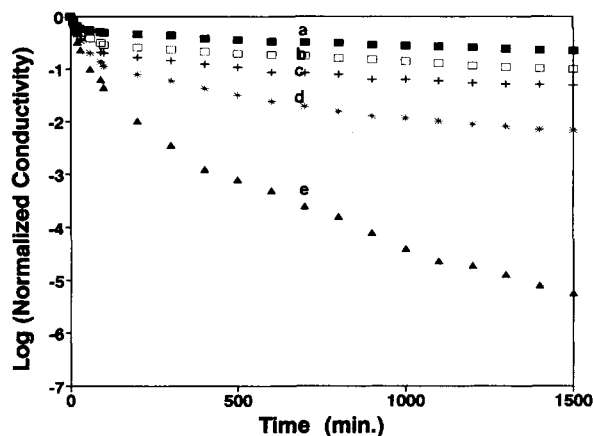


**Figure 2** Conductivity stability of BSA-doped PAN-N composite films at elevated temperatures: (a) 80°C, (b) 95°C, (c) 110°C, (d) 125°C, and (e) 150°C.

$$d\sigma/dt = k \Delta\sigma \quad (1)$$

$$k = A \exp(-E_A/RT)$$

$$\log k = \log A - (E_A/2.303R)(1/T) \quad (2)$$

where  $k$  is the conductivity degradation rate constant,  $E_A$  is the activation energy for the conductivity degradation process;  $R$  and  $T$  are the gas constant ( $8.314 \times 10^{-3}$  kJ/Kmol) and temperature in Kelvin, respectively.

It was found that the stability of organic-acid-doped PAN-N composite films is better than that of inorganic-acid-doped materials. The conductivity stability of these PAN-N composite films have the following order: BSA-doped > SSA-doped > TSA-doped > HCl-doped. As seen in the Figures 1-4,

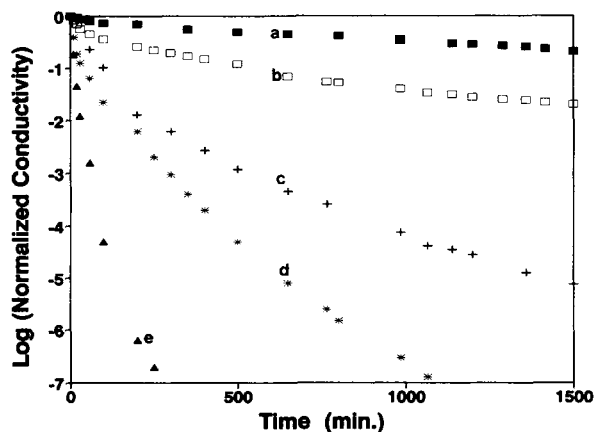


**Figure 3** Conductivity stability of SSA-doped PAN-N composite films at elevated temperatures: (a) 80°C, (b) 95°C, (c) 110°C, (d) 125°C, and (e) 150°C.

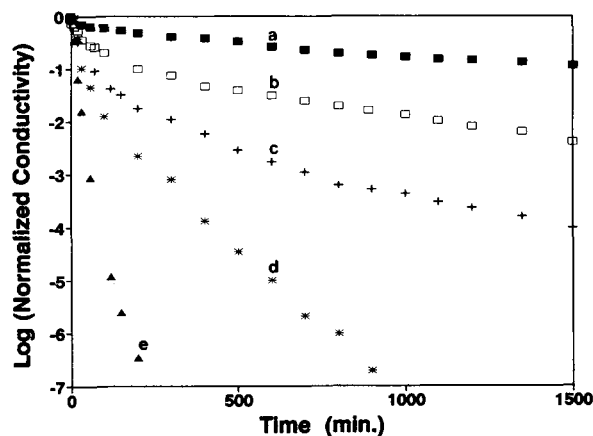


**Figure 4** Conductivity stability of TSA-doped PAN-N composite films at elevated temperatures: (a) 80°C, (b) 95°C, (c) 110°C, (d) 125°C, and (e) 150°C.

the thermal stability of conductivity for all of the PAN-N composite films is strongly dependent on the nature of the dopant species introduced during the polymerization. It seems that this is due to the thermal and environmental stability of the dopant species and physicochemical interactions between the dopant anions and the charged polymer chains, etc. These are in good agreement with the ultraviolet-visible spectroscopic results.

By performing Arrhenius analysis [Eqs. (2) and (3)], we assumed first-order reaction kinetics. However, as seen in Figure 5, all of the plots of  $\ln k$  vs.  $1/T$  did not give linear results ( $r^2 > 0.99$ ) in calculating the activation energies. The conductivity degradation kinetic behaviors of the PAN-N composite films doped with SSA and TSA were first order, but those of HCl- and BSA-doped PAN-N films were not. The nonlinear kinetic behavior of HCl- and BSA-doped PAN-N films were found to be in contrast to that of polyaniline film itself.<sup>20</sup> The nonlinear kinetic behavior suggests that multiple mechanisms of degradation or multiorder reactions are operating in the PAN-N composite films doped with HCl and BSA.

Since the degradation behavior of the PAN-N composite films doped with SSA and TSA follow first-order kinetics, we can calculate the activation energy for the degradation process from Eq. (3) and the slope of the line as shown in Figure 5. The calculated activation energies of the PAN-N composite films doped with SSA and TSA are 71.4 and 69.3 kJ/mol, respectively. Knowing the activation energy and a rate constant for the degradation at a specific temperature, we can calculate a rate constant for the degradation of the conductivity at room

**Table I** Conductivity at Room Temperature and Re-doped Conductivity after Thermal Treatment and Rate Constants of Degradation for Various Doped PAn-N Composite Films

Sample	Conductivity at 25°C (S/cm)	Temperature (°C)	Rate Constant, $K$ ( $\text{min}^{-1}$ )	Re-doped Conductivity <sup>a</sup> (S/cm)
HCL PAn-N	0.726	80	$1.88 \times 10^{-3}$	$1.11 \times 10^{-3}$
		95	$2.40 \times 10^{-3}$	
		110	$3.04 \times 10^{-3}$	
		125	$6.83 \times 10^{-3}$	
		150	$3.50 \times 10^{-2}$	
BSA PAn-N	0.534	80	$2.45 \times 10^{-4}$	$2.03 \times 10^{-2}$
		95	$3.20 \times 10^{-4}$	
		110	$4.40 \times 10^{-4}$	
		125	$8.60 \times 10^{-4}$	
		150	$2.85 \times 10^{-3}$	
SSA PAn-N	0.379	80	$3.60 \times 10^{-4}$	$1.98 \times 10^{-2}$
		95	$8.80 \times 10^{-4}$	
		110	$2.22 \times 10^{-3}$	
		125	$5.10 \times 10^{-3}$	
		150	$2.01 \times 10^{-2}$	
TSA PAn-N	0.103	80	$4.94 \times 10^{-4}$	$3.16 \times 10^{-3}$
		95	$1.10 \times 10^{-3}$	
		110	$2.64 \times 10^{-3}$	
		125	$6.10 \times 10^{-3}$	
		150	$2.45 \times 10^{-2}$	

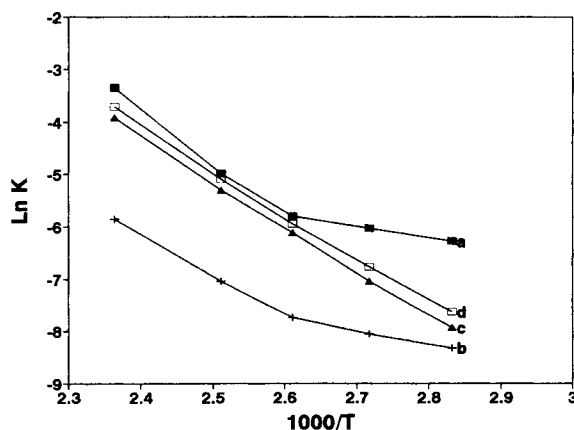
<sup>a</sup> Conductivity re-doped in each protonic acid solution after thermal treatment at 180°C for 2 h.

temperature. The calculated rate constants of the PAn-N composite films doped with SSA and TSA are  $2.48 \times 10^{-6}$  and  $3.68 \times 10^{-6} \text{ min}^{-1}$ , respectively.

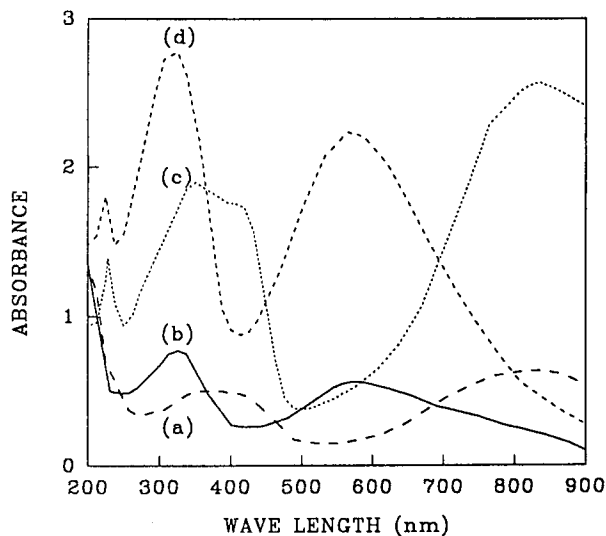
### Spectroscopic and Thermal Studies

Figure 6 shows the ultraviolet-visible spectra of the two different forms of PAn-N composite films and the polyaniline coated on the quartz plate. Figures 6(a) and (c) represent the spectra of the as-prepared doped forms. The absorption band at 353 nm is a  $\pi-\pi^*$  transition and the absorbances at 418 and 830 nm arise from the polaron band transitions.<sup>21</sup> The absorption peak at 229 nm in the PAn-N composite film [Figs. 6(c) and (d)], which did not exist in pristine polyaniline, is due to aniline monomer remaining in the inner side of composite films. It is thought that the remaining monomers may have an effect on the physical and mechanical properties of PAn-N composite films. The detailed study of the physical and dynamic mechanical properties of the composite films will be reported in a future study. Figures 6(b) and (d) represent the spectra of the emeraldine base forms of polyaniline obtained by immersing as-prepared doped polyaniline and PAn-N in 0.5 mol %

KOH solution. The absorption bands at about 323 and 570 nm represent the  $\pi-\pi^*$  transition and the excitation band of the quinoid ring, respectively.<sup>21</sup> As shown in Figure 6, it seems that there is little difference of ultraviolet-visible spectra between the



**Figure 5**  $\ln K$  vs.  $1/T(K)$  for various doped PAn-N composite films. Rate constants,  $K$ , are from Table I: (a) HCl-doped PAn-N, (b) BSA-doped PAn-N, (c) SSA-doped PAn-N, and (d) TSA-doped PAn-N.



**Figure 6** Ultraviolet-visible spectra of polyaniline and PAN-N doped with HCl: (a) polyaniline doped with HCl, (b) polyaniline de-doped in aqueous 0.5 mol % KOH solution, (c) PAN-N doped with HCl, and (d) PAN-N de-doped in aqueous 0.5 mol % KOH solution.

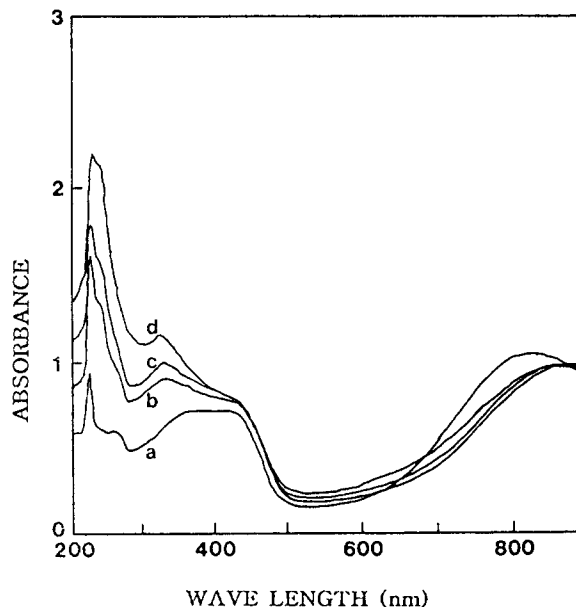


**Figure 8** Ultraviolet-visible spectra of BSA-doped PAN-N composite films with various thermal de-doping times: (a) 0 min, (b) 30 min, (c) 60 min, and (d) 120 min.

PAN-N film and pristine polyaniline except the absorption peak at 229 nm. A set of ultraviolet-visible spectra of PAN-N composite films doped with various dopants are shown with thermal de-doping time at 150°C in Figures 7-10. These spectra were re-

corded at room temperature after heating the composite films. Figure 7 shows the changes of the absorption spectra of the HCl-doped PAN-N composite film with thermal de-doping time at 150°C. When the thermal de-doping time is gradually increased

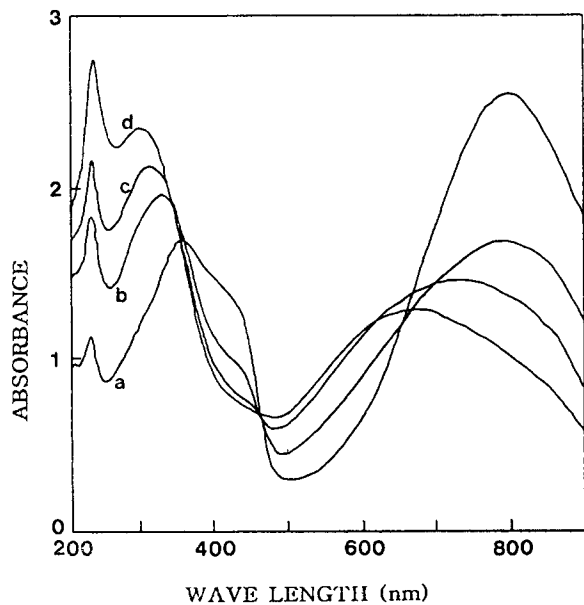


**Figure 7** Ultraviolet-visible spectra of HCl-doped PAN-N composite films with various thermal de-doping times: (a) 0 min, (b) 30 min, (c) 60 min, and (d) 120 min.

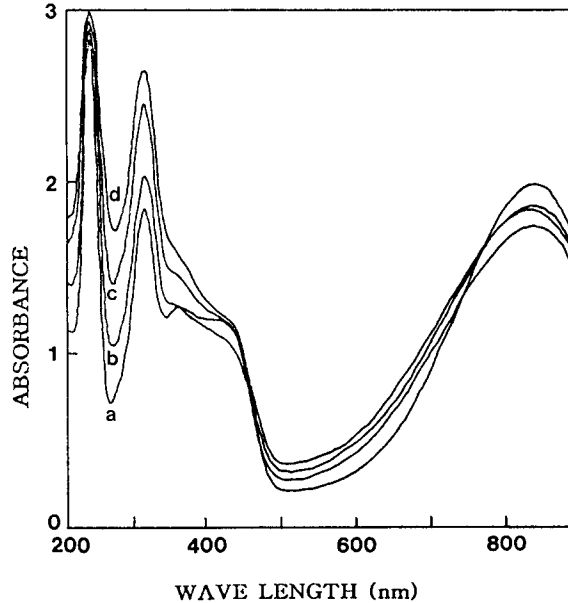


**Figure 9** Ultraviolet-visible spectra of SSA-doped PAN-N composite films with various thermal de-doping times: (a) 0 min, (b) 30 min, (c) 60 min, and (d) 120 min.

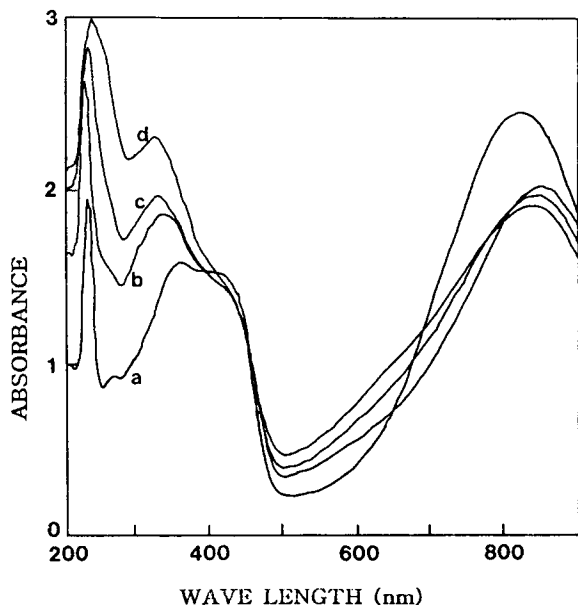


**Figure 10** Ultraviolet-visible spectra of TSA-doped PAN-N composite films with various thermal de-doping times: (a) 0 min, (b) 30 min, (c) 60 min, and (d) 120 min.

from 0 to 120 min, the three-band spectrum of the doped form, except the band at 229 nm, which is due to the remained monomer in the composite film, is changed to a two-band spectrum which is found in the emeraldine base form of polyaniline. Upon thermal de-doping, the two polaron absorption bands at 423 and 800 nm is gradually diminished whereas the excitation band appears at 670 nm, and the  $\pi-\pi^*$  transition peak at 353 nm is increased and shifts to the lower wavelength. Concurrent with these spectral changes is a dramatic drop in the electrical conductivity of the PAN-N composite film. Similar changes are also observed for the PAN-N composite films doped with different dopants, although the extents of the spectral changes and conductivity drops are moderate at that temperature (Figs. 8–10). It is interesting to note that the peak associated with the  $\pi-\pi^*$  transition has shifted to higher energies relative to that observed in the PAN-N composite film, which is de-doped in 0.5 mol % KOH solution [Fig. 6(d)]. This would suggest that thermal treatment of the doped PAN-N composite films, in addition to reversing the doping process, also regenerates the polyaniline of the composite system in a more disordered form and hence develops a less effective conjugation length. These results are opposite to that of  $\text{FeCl}_3$ -doped poly(3-hexylthiophene) film.<sup>18</sup> This effect is most pronounced in HCl-doped PAN-N composite film. The

reestablishment of the  $\pi-\pi^*$  transition band, which has essentially equal intensity to the PAN-N de-doped in KOH solution, indicates that the thermal de-doping process takes place without major structural modifications of the polyaniline in the composite system. A re-doping experiment on thermally de-doped PAN-N composite film was carried out to support this assumption (Table I). In this case it was found that the re-doped conductivities of all of the thermal de-doped PAN-N composite films were lower than their original values. These results might be partially explained by previously mentioned disorder of the polyaniline in the composite system. Therefore, the thermal de-doping process is not completely reversible.

The DSC thermograms of the PAN-N composite films doped with various protonic acids are shown in Figure 11. The thermogram of a pristine Nylon 6 film is also included in this figure for comparison. Table II shows the heat of fusion ( $\Delta H_f$ ), melting temperature, and the degree of crystallinity ( $X_c$ ) of various composite films. As seen in Table II,  $\Delta H_f$  and  $X_c$  of the composite films are somewhat reduced by the polymerization of polyaniline in Nylon 6 film

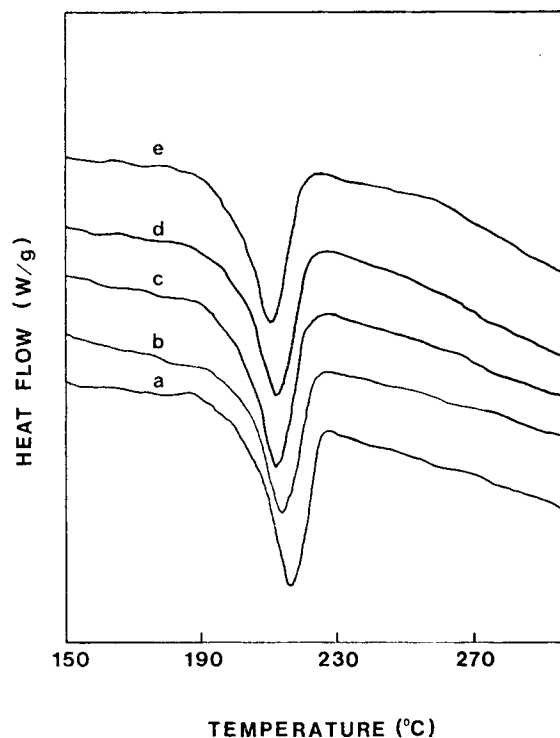


**Figure 11** DSC thermograms of PAN-N composite films with various protonic acids: (a) pristine Nylon 6 film, (b) HCl-doped PAN-N, (c) BSA-doped PAN-N, (d) SSA-doped PAN-N, and (e) TSA-doped PAN-N.

**Table II Heat of Fusion, Melting Temperature, and Crystallinity of Various Doped PAN-N Composite Films**

Sample	Heat of Fusion, $\Delta H_f$ (J/g)	Melting Point, $T_m$ ( $^{\circ}$ C)	Crystallinity, $X_c$ (%)
Nylon 6	55.28	217.4	21.0
HCL PAN-N	49.40	215.5	18.7
BSA PAN-N	50.32	212.4	19.1
SSA PAN-N	48.82	213.1	18.5
TSA PAN-N	45.38	211.0	17.2

compared to Nylon 6. Also, the Nylon 6 melting point ( $T_m$ ) tends to shift to slightly lower temperature in the composite film. This indicates that the crystal structure of Nylon 6 in the composite film is not greatly affected by the presence of polyaniline. These observations are consistent with previously reported results.<sup>14,15</sup>

## CONCLUSIONS

The conductivity stability of organic-acid-doped PAN-N composite films is better than for inorganic-acid-doped materials. The nature of the dopant introduced into the polyaniline during polymerization has a significant influence on the conductivity stability of the composite films. Two different degradation kinetic processes of electrical conductivity are found depending on the species of protonic acids. The conductivity degradation of PAN-N composite films doped with SSA and TSA is found to obey first-order reaction kinetics, while that of the other dopants follows multiorder kinetics. From the spectroscopic results, the thermal de-doping process of the doped PAN-N composite films, which reverses the doping process, takes place without major structural modifications of the polyaniline in the composite system. However, the possibility of changes of physical properties of polyaniline, such as a development of a disordered form, cannot be excluded. The crystal structure of Nylon 6 in the composite films is slightly affected by the formation of polyaniline; the degree of perturbation (by DSC) is somewhat dopant-dependent.

This work was carried out under a research grant from the Korea Science and Engineering Foundation (9223-0006).

## REFERENCES

1. J. P. Travers, J. Chroboczek, F. Deverux, F. Genoud, and M. Nechtschrein, *Mol. Cryst. Liq. Cryst.*, **121**, 195 (1985).
2. A. G. MacDiarmid, J. C. Chiang, A. F. Richter, and A. J. Epstein, *Synth. Met.*, **18**, 285 (1987).
3. G. Gustafsson, Y. Cao, G. M. Treacy, F. Klaretter, N. Colaneri, and A. J. Heeger, *Nature (London)*, **357**, 977 (1992).
4. S. K. Dhawan and D. C. Trivedi, *Polym. Int.*, **25**, 55 (1991).
5. A. G. MacDiarmid, J. C. Chiang, M. Halpern, W. L. Mu, N. L. D. Somasiri, W. Wu, and S. I. Yaniger, *Mol. Cryst. Liq. Cryst.*, **121**, 173 (1985).
6. A. Andreatta, Y. Cao, J. C. Chiang, P. Smith, and A. J. Heeger, *Synth. Met.*, **26**, 383 (1988).
7. J. R. Reynolds, C. K. Baker, and M. Gieselman, *Polym. Prepr.*, **30**, 151 (1989).
8. B. D. Malhotra, S. Ghosh, and R. Chandra, *J. Appl. Polym. Sci.*, **40**, 1049 (1990).
9. S.-A. Chen and W.-G. Fang, *Macromolecules*, **24**, 1242 (1991).
10. J. M. Ginder, A. J. Epstein, and A. G. MacDiarmid, *Synth. Met.*, **37**, 45 (1990).
11. T. Hagiwara, M. Yamaura, and K. Iwata, *Synth. Met.*, **25**, 243 (1988).
12. V. G. Kulkatni, L. D. Campbell, and W. R. Mathew, *Synth. Met.*, **30**, 321 (1989).
13. Y. Wei and K. F. Hsueh, *J. Polym. Sci., Part A: Polym. Chem.*, **27**, 4351 (1990).
14. S. W. Byun and S. S. Im, *Synth. Met.*, **57**, 3501 (1993).
15. S. W. Byun and S. S. Im, *J. Appl. Polym. Sci.*, **51**, 1221 (1994).
16. L. A. Samuelson and M. A. Druy, *Macromolecules*, **19**, 824 (1986).
17. M. Salmon, A. F. Diaz, A. J. Logan, M. Krounbi, and J. Bargon, *Mol. Cryst. Liq. Cryst.*, **83**, 295 (1982).
18. Y. Wang and M. F. Rubner, *Synth. Met.*, **39**, 153 (1990).
19. M. Osagawa, K. Funahashi, T. Demura, T. Hagiware, and K. Iwata, *Synth. Met.*, **14**, 61 (1986).
20. Y. Wang and M. F. Rubner, *Synth. Met.*, **47**, 255 (1992).
21. M. Wan, *Synth. Met.*, **31**, 51 (1989).

Received March 15, 1994

Accepted July 18, 1994